Journal of ELECTRONIC MATERIALS, Vol. 41, No. 8, 2012
DOI: 10.1007/s11664-012-2038-1
© 2012 TMS

# High-Temperature Oxidation Behavior of Filled Skutterudites $Yb_yCo_4Sb_{12}$

XUGUI XIA,[1] PENGFEI QIU,[1,2] XUN SHI,[1] XIAOYA LI,[1] XIANGYANG HUANG,[1] and LIDONG CHEN[1]

1.—CAS Key Laboratory of Materials for Energy Conversion, Shanghai Institute of Ceramics, Chinese Academy of Sciences, 1295 DingXi Road, Shanghai 200050, China. 2.—e-mail: qiupf@mail.sic.ac.cn

The oxidation behavior of filled skutterudites $Yb_yCo_4Sb_{12}$ was investigated. The overall oxidation of $Yb_yCo_4Sb_{12}$ consists of two stages. In the first stage, densified oxide layers form on the surface gradually due to the reaction between oxygen and skutterudite at high temperature. In the second stage, microcracks evolve in the oxide layers because of mismatch of coefficient of thermal expansion between the oxide layer and skutterudite matrix, which accelerates the oxidation by providing transport paths for both outside oxygen and inside Sb. The overall oxidation process can be described through the repetitive cycle: dense layer formation → stress release → microcrack formation → self-repair → dense layer formation. The oxidation activation energy of filled skutterudites determined using thermogravimetry method with multi-heating rates is lower than that of unfilled $CoSb_3$. Moreover, it was found that, with increasing Yb filling fraction, the oxidation activation energy decreases monotonically. Our results suggest that protection against oxidation is necessary for application of filled skutterudites.

**Key words:** Thermoelectric, skutterudite, oxidation, activation energy

## INTRODUCTION

Recently, thermoelectric materials have attracted considerable interest because of their potential applications in power supply and sustainable energy management.[1–5] The thermoelectric figure of merit ($ZT$) is an important parameter in evaluating thermoelectric materials. It determines the conversion efficiency of thermoelectric devices, with high $ZT$ being favorable for high conversion efficiency. However, the durability of thermoelectric materials under operating conditions also has to be considered in real, long-term operation scenarios.

$CoSb_3$-based filled skutterudites are some of the most promising thermoelectric materials for operation at elevated temperature. In the past decade, various filled $R_yCo_4Sb_{12}$ compounds have been synthesized,[6–9] with a maximum $ZT$ value of 1.7 being reported.[10] However, the question of long-term stability in real applications has not been well studied so far, and deep understanding of this issue is lacking, for example, the impact of fillers and filling fraction on thermal stability, etc. Because most of the fillers are alkali, alkaline-earth, or rare-earth elements which have high oxygen affinity, the thermal stability of filled skutterudites at elevated temperature in air could be significantly reduced. Moreover, the enlarged $Co_4Sb_{12}$ framework and increased lattice parameter resulting from filling could influence the chemical bonds between Co and Sb atoms[11] as well and thus affect the oxidization behavior of skutterudites. Therefore, clear understanding of the impact of fillers and filling fraction on thermal stability is necessary and urgently needed for application of filled skutterudites.

Antioxidation ability is one of the most important factors to evaluate the thermal stability of filled skutterudites considering their high operation temperatures.[12–17] Generally, antioxidation capability

(Received November 29, 2011; accepted March 1, 2012; published online April 3, 2012)

can be described using the oxidation activation energy ($E_a$), where larger $E_a$ indicates greater stability against oxygen. In this paper, the oxidation behavior of filled skutterudites $Yb_yCo_4Sb_{12}$ with different filling fractions ($y$ = 0, 0.2, 0.3, and 0.4) and at different temperature ranges was systematically studied. The thermogravimetry method with multi-heating rates was used to calculate $E_a$. Our results show that the overall oxidation of $Yb_yCo_4Sb_{12}$ consists of two stages with different oxidation mechanisms and moreover that $E_a$ decreases with increasing Yb filling fraction, revealing the degraded antioxidation ability of filled skutterudites.

## EXPERIMENTAL PROCEDURES

### Synthesis

High-purity raw materials Yb (ingot, 99.99%), Co (bulk, 99.985%), and Sb (shot, 99.9999%) were weighed out at designed atomic ratios and sealed in evacuated quartz ampoules with coated carbon. The sealed ampoules were slowly heated up to 1350 K and kept for 10 h, then quenched in a water bath and annealed at 1073 K for 7 days. The ingots were ground into fine powder (160–200 mesh), and bulk samples with relative density greater than 95% were achieved by 10 min to 15 min spark plasma sintering (SPS) at 873 K. The phase purity of the samples was checked by x-ray diffraction (XRD, Rigaku, Rint2000) and electron probe microanalysis (EPMA, JEOL, JXA-8100) with energy-dispersive spectroscopy (EDS). All powder and bulk samples were identified as having single-phase cubic $Co_4As_{12}$ skutterudite structure.

### XRD, EPMA, and SEM Analyses

$Yb_yCo_4Sb_{12}$ powder samples (160–200 mesh) were heated from room temperature to the assigned oxidation temperature (650 K, 750 K, 800 K, 850 K, 900 K, and 923 K) with heating rate of 5 K/min, and then cooled down to room temperature. XRD was used to check the oxidation products. For $Yb_yCo_4Sb_{12}$ bulk samples, the corresponding oxidation temperatures were 750 K, 800 K, and 900 K, respectively. Microstructure and compositional analysis were carried out on oxidized samples using SEM and EDS.

### Thermogravimetry and Derivative Thermogravimetry Measurements

Thermogravimetry (TG) and derivative thermogravimetry (DTG) analysis on $Yb_yCo_4Sb_{12}$ powder samples were performed on a thermal analysis instrument (TGS-2A) in static air with heating rates $\beta$ of 5 K/min, 10 K/min, and 15 K/min, respectively. The same batch of powder was used for both TG/DTG and XRD testing to ensure reliable results. For comparison, a 5 K/min heating rate corresponding to the oxidation process was used in the XRD analysis. The amount of sample for each measurement was 200 mg, and the measurement temperature ranged from 300 K to 923 K. The system was calibrated without a sample loaded using the same heating procedure prior to the experiments. Reproducibility was ensured by multiple measurements at the same heating rate.

## RESULTS AND DISCUSSION

All our measurement (XRD, EPMA, SEM, and TG/DTG) showed similar oxidation behavior for samples with different Yb filling fractions, so $Yb_{0.3}Co_4Sb_{12}$ is used as a typical example to discuss the oxidation process below.

Figure 1 shows the XRD patterns for the $Yb_{0.3}Co_4Sb_{12}$ powder sample after oxidation at different temperatures. For the sample with oxidation temperature below 650 K, no oxide was observed in the XRD pattern. The diffraction peaks of $Sb_2O_3$ appear as the temperature increases to 750 K, and peak intensity is greatly enhanced for sample oxidized at 800 K. Above 800 K, more oxides such as $Yb_2O_3$, $Sb_2O_3$, $\alpha$-$Sb_2O_4$, $\beta$-$Sb_2O_4$, $CoSb_2O_4$, and $CoSb_2O_6$ appear, with no further new oxides being observed in the XRD patterns at oxidation temperatures above 900 K. Compared with oxidation of unfilled $Co_4Sb_{12}$, the only difference is the generation of $Yb_2O_3$ in Yb-filled samples. The observation of the same relationship between oxidation temperature and oxide phases in samples with different Yb filling fractions indicates that they have similar oxidation mechanisms. From the phase diagram, $Co_4Sb_{12}$ is stable below the peritectic decomposition temperature (1147 K), which is much higher than the maximum oxidation temperature (923 K) used in our experiment, so we consider the reaction of skutterudite with oxygen to be the main reason for the formation of oxide phases, rather than skutterudite decomposition.

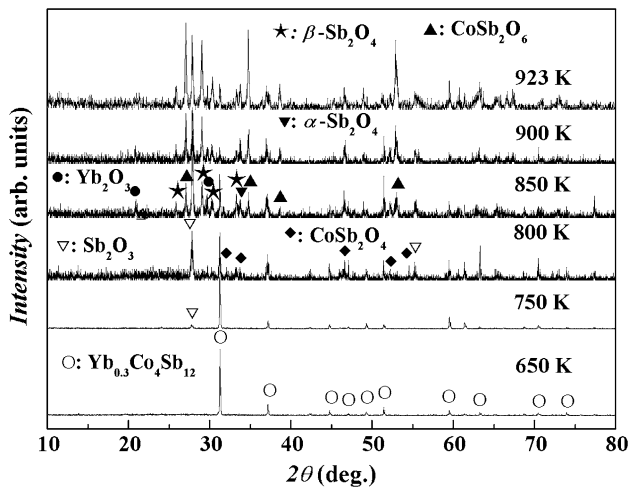


Fig. 1. XRD patterns for $Yb_{0.3}Co_4Sb_{12}$ powder samples oxidized at different temperatures with main peaks of oxides marked.

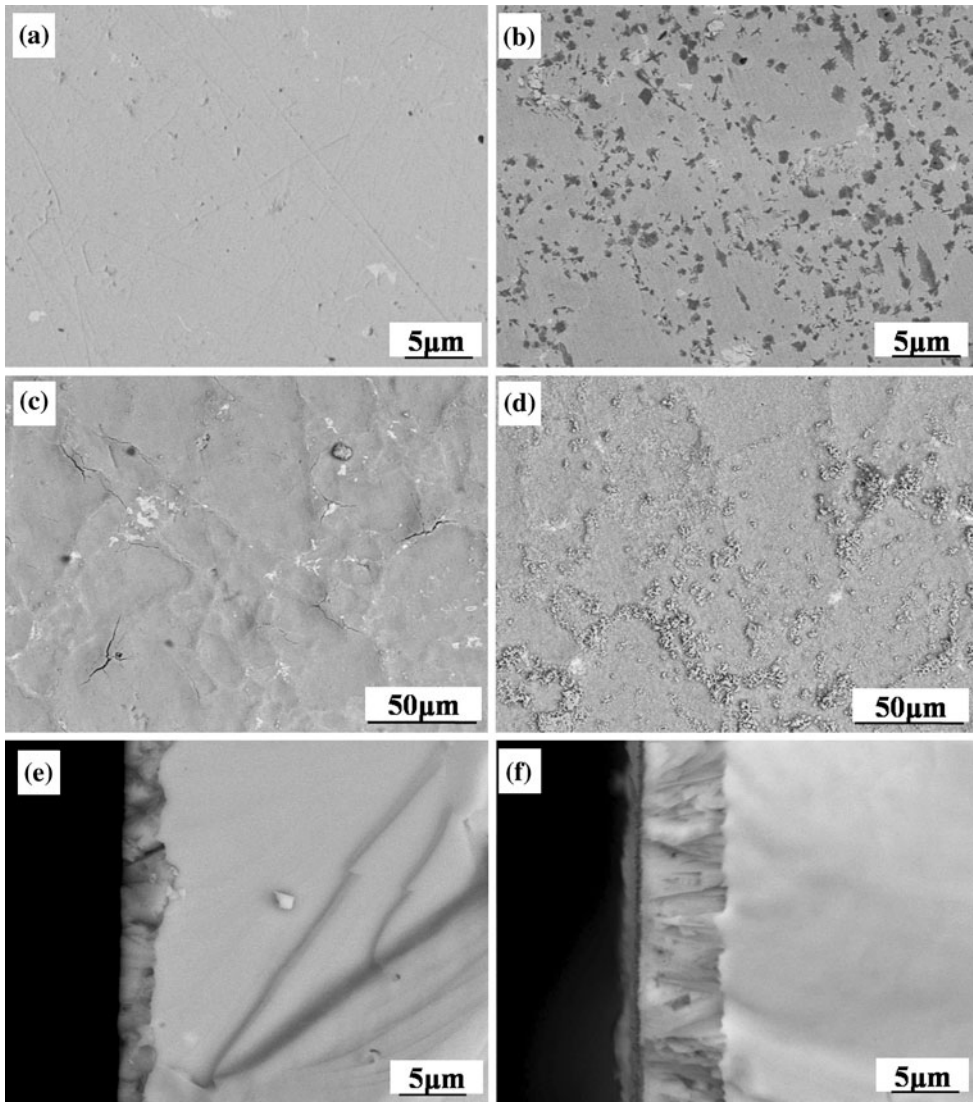


Fig. 2. Backscattered electron images for $Yb_{0.3}Co_4Sb_{12}$ filled skutterudites: (a) without oxidation, (b–d) after 3 h oxidation in air at 750 K, 800 K, and 900 K, and (e, f) cross-section views of samples in (c) and (d).

The morphology and microstructure of oxidized $Yb_{0.3}Co_4Sb_{12}$ bulk samples were examined by SEM. As shown in Fig. 2a, the original sample is single skutterudite phase with all elements distributed homogeneously in the matrix. After oxidation at 750 K for 3 h in air, many gray areas evolved on the sample surface (Fig. 2b), being identified as oxygen-rich phase by EDS and suggesting the presence of oxides. From Fig. 2c and the corresponding cross-section image in Fig. 2e for the sample oxidized at 800 K for 3 h, it is clearly seen that a dense layer is formed on the sample surface. The composition of the layer is identified as 17.3 at.% Co, 40.1 at.% Sb, 0.8 at.% Yb, and 41.8 at.% O. Microcracks are also found in this oxide layer, which we believe to be generated due to the mismatch of coefficient of thermal expansion (CTE) between the oxide layer (e.g., $Sb_2O_3$: $19.7 \times 10^{-6}$ $K^{-1}$, $Yb_2O_3$: $6.1 \times 10^{-6}$ $K^{-1}$ at room temperature) and $Yb_yCo_4Sb_{12}$ skutterudite matrix ($9 \times 10^{-6}$ $K^{-1}$ to $10 \times 10^{-6}$ $K^{-1}$).[18,19] On the other hand, the accelerated penetration of oxygen into bulk material as a result of the microcracks leads to continuous growth of the oxide layer. Meanwhile, further sublimated Sb from inside the skutterudite can form Sb-containing oxides on top of the first oxide layer, promoting the formation of a bilayer oxidation structure as shown in Fig. 2d, f.[20] In addition, the unstable $Sb_2O_3$ in the first layer would decompose into $Sb_2O_4$ and Sb at high temperature.[21] This part of Sb can also diffuse through the first oxide layer and react with oxygen, which is believed to be another reason for the formation of the outer oxide layer.

TG curves for $Yb_{0.3}Co_4Sb_{12}$ powders at different heating rates are shown in Fig. 3. Here, the relative change of total weight ($\Delta W$) is defined as $(W - W_0)/W_0$ with $W$ the weight during oxidation and $W_0$ the initial weight. At temperature below 700 K, $\Delta W$ is

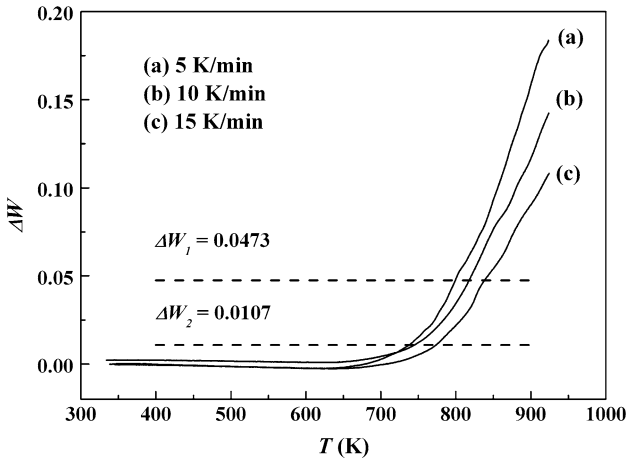


Fig. 3. TG curves for $Yb_{0.3}Co_4Sb_{12}$ with different heating rates in air: (a) 5 K/min, (b) 10 K/min, and (c) 15 K/min. Dashed line marks $\Delta W$ of 0.0107 and 0.0473, respectively.

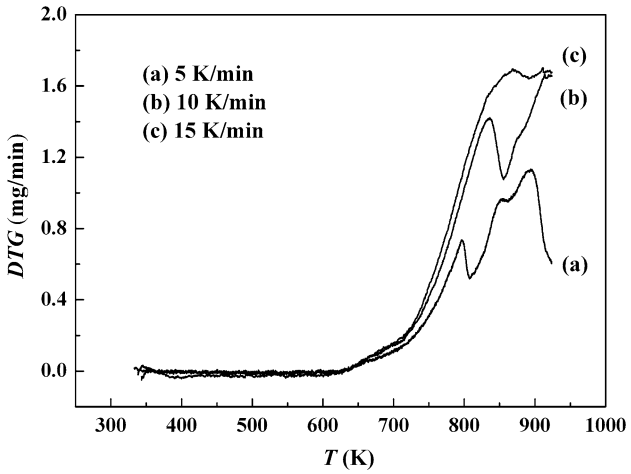


Fig. 4. DTG curves for $Yb_{0.3}Co_4Sb_{12}$ in air with different heating rates: (a) 5 K/min, (b) 10 K/min, and 15 K/min.

almost unchanged, consistent with previous reports that oxidation of $Co_4Sb_{12}$ starts at temperature above 673 K in air.[13,17] As the temperature goes above 700 K, $\Delta W$ increases significantly, which is related to the increase of oxidation products.

The corresponding DTG curves for $Yb_{0.3}Co_4Sb_{12}$ powders with different heating rates are shown in Fig. 4. Two peaks at temperature above 700 K are observed for heating rate of 5 K/min. Combined with the previous XRD and SEM analysis, this indicates that there are two oxidation stages with different mechanisms involved in the process. At the beginning of the first stage, the oxidation rate increases as the temperature increases, corresponding to the raised part of the DTG curve. This is due to the continuous, fast reaction between oxygen and skutterudite. As densified oxide layers form on the sample surface, oxygen penetration is suppressed, which correspondingly leads to an evident DTG reduction after the first peak. In addition, the formation of new oxides at temperature above 800 K may also block oxygen penetration and slow down the oxidation process. In the second stage, as the temperature is further increased, microcracks evolve in the densified oxide layers due to release of the large stress generated by the CTE mismatch between the oxide layer and skutterudite matrix. Then, the suppressed oxidation process will recover due to accelerated transport of oxygen and Sb through the cracks. Meanwhile, Sb sublimated through these cracks could continue to react with penetrated oxygen. Formation of new oxides will gradually fill the cracks and cause oxidation suppression again through this self-repair behavior (Fig. 2d, f). This is confirmed by the DTG decrease after reaching the second peak. As the temperature is further increased, the oxide layer will continue to grow. Stress accumulates and leads to the appearance of microcracks when the newly formed oxide layer grows thick enough. The whole oxidation process of $Yb_{0.3}Co_4Sb_{12}$ in air can be described by the following repetitive cycle: dense layer formation → stress release → microcrack formation → self-repair → dense layer formation.

Besides temperature, oxidation time is another important factor affecting the oxidation cycle mentioned above. From Fig. 4 we can see that the number of peaks in the DTG curve increases with decreasing heating rate. This implies that more oxidation cycles happen at lower heating rate, which means longer oxidation time on the other hand. In this case, thicker oxide layer and more accumulated stress would cause more microcracks to be generated, which can be confirmed by extending the oxidation time of $Yb_{0.3}Co_4Sb_{12}$ bulk as shown by the results in Fig. 5 (for 7 h at 900 K). It is easy to see that there are more Sb-oxide particles on the surface compared with the sample oxidized for 3 h at the same temperature (Fig. 2d). These particles mainly accumulate in microcrack areas. It can be found from Fig. 5b that the microcracks have already spread into the $Yb_{0.3}Co_4Sb_{12}$ matrix. The thicker oxide layer near the microcracks indicates more active oxidation around these areas due to enhanced diffusion of oxygen and Sb through these microcracks. One can also see a long crack underneath the oxide layer in Fig. 5b, which may be caused by the large stress arising from the CTE mismatch between the skutterudite and oxide layers. Through such cracks, oxygen can easily penetrate into the inner part of the bulk and further deteriorate the skutterudite.

Based on TG and DTG measurements, $E_a$ can be calculated by the thermogravimetry method with multi-heating rates. This method has been extensively used in other systems (e.g., superconductors)[22,23] but has never been applied in thermoelectric materials. The advantage of this method is that one does not have to know the exact chemical reaction or reaction time. In the present study, we assume that

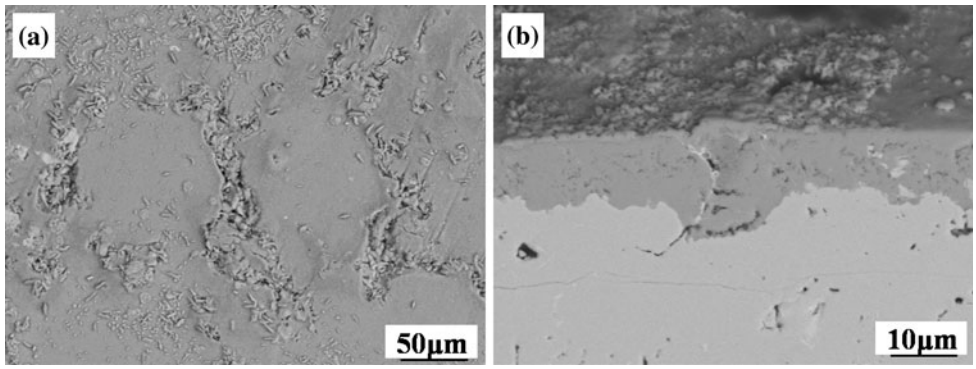


Fig. 5. Backscattered electron images for $Yb_{0.3}Co_4Sb_{12}$ oxidized in air for 7 h at 900 K: (a) surface view and (b) cross-sectional view. Sample is tilted in (b) for observation of both surface and cross-section.

the oxidation of $Yb_yCo_4Sb_{12}$ filled skutterudites obeys the Arrhenius equation

$$\beta\frac{d\alpha}{dt} = Ae^{E_a/RT}f(\alpha), \quad (1)$$

where $\beta$ is the heating rate, $d\alpha/dt$ is the reaction rate, $A$ is the pre-exponential factor, which is normally taken as constant, $R$ is the gas constant, and $T$ represents the absolute temperature. $\alpha = (W_t - W_0)/(W_\infty - W_0)$ is the fractional weight, where $W_\infty$ is the sample weight at infinite time after reaction completion. $f(\alpha)$ is a function of $\alpha$, and the expression depends on the oxidation mechanism. Equation 1 can be rewritten as follows by taking the natural logarithm of both sides:

$$\ln\left(\beta\frac{d\alpha}{dt}\right) = \ln(A\cdot f(\alpha)) - \frac{E_a}{R}\cdot\frac{1}{T}. \quad (2)$$

Replacing $\alpha$ with $(W_t - W_0)/(W_\infty - W_0)$, we have

$$\mathrm{In}\left(\beta\frac{dW_t}{dt}\right) = \mathrm{In}(A\cdot f(\alpha)) - \frac{E_a}{R}\cdot\frac{1}{T} + \mathrm{In}(W_\infty - W_0). \quad (3)$$

Here, $\beta dW_t/dt$ is given by the DTG values, so the equation can be rewritten as

$$\ln(\mathrm{DTG}) = \ln(A\cdot f(\alpha)) - \frac{E_a}{R}\cdot\frac{1}{T} + \ln(W_\infty - W_0), \quad (4)$$

where $\ln[A\cdot f(\alpha)]$ and $\ln(W_\infty - W_0)$ are assumed to be constant and independent of temperature. $E_a/R$ is the slope of ln(DTG) versus $1/T$.

Two examples are given in Fig. 6. With given $\Delta W_1 = 0.0107$, ln(DTG) versus $1/T$ is obtained by fitting three TG curves in Fig. 3 with corresponding temperatures, DTG values, and heating rates of: 737.1 K, 0.245 mg/min, and 5 K/min; 748.3 K, 0.395 mg/min, and 10 K/min; and 773.4 K, 0.758 mg/min, and 15 K/min, respectively. Thus, $E_a$ is calculated to be about 144 kJ/mol in the temperature range from 737.1 K to 773.4 K. With given $\Delta W_2 = 0.0473$, we get $E_a$ of 113 kJ/mol at temperatures from 799.1 K to 837.9 K. Using the same

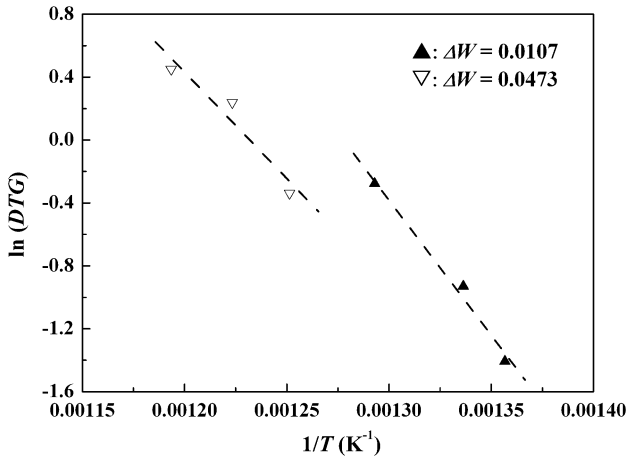


Fig. 6. ln(DTG) as a function of $1/T$ for $Yb_{0.3}Co_4Sb_{12}$ at $\Delta W$ of 0.0107 and 0.0473, respectively.

method, $E_a$ for the $Yb_{0.3}Co_4Sb_{12}$ sample at different temperature ranges was calculated and is listed in Table I, with values around 140 kJ/mol to 150 kJ/mol at temperature below 800 K, and 105 kJ/mol to 115 kJ/mol at temperature above 800 K. This decrease at high temperature could be attributed to different oxidation mechanisms. For temperatures below 800 K, oxidation areas grow slowly from spots to dense layers with high activation energy and low oxidation speed, whereas the formation of new oxides and generation of microcracks at temperature higher than 800 K decrease the activation energy and speed up the oxidation.

Calculated $E_a$ values for all $Yb_yCo_4Sb_{12}$ with different Yb filling fractions at different temperature ranges are shown in Fig. 7. For unfilled $Co_4Sb_{12}$, $E_a$ is about 170 kJ/mol and almost independent of temperature, which is consistent with the reported value of 160 ± 21 kJ/mol obtained by the isothermal oxidation method.[13] The obvious decrease of $E_a$ as the filling fraction increases suggests that samples with higher Yb content are more easily oxidized in air. This is understandable considering the high oxygen affinity of Yb atoms and the weak bonding of Yb to the

**Table I. Oxidation activation energy calculation for $Yb_{0.3}Co_4Sb_{12}$**

| | 5 K/min | | 10 K/min | | 15 K/min | | |
|---|---|---|---|---|---|---|---|
| $\Delta W$ | $T$ (K) | DTG | $T$ (K) | DTG | $T$ (K) | DTG | $E_a$ (kJ/mol) |
| 0.0107 | 737.1 | 0.245 | 748.3 | 0.395 | 773.4 | 0.758 | 144 |
| 0.0157 | 751.1 | 0.322 | 761.7 | 0.527 | 785.1 | 0.931 | 148 |
| 0.0221 | 766.9 | 0.435 | 777.6 | 0.711 | 798.3 | 1.122 | 148 |
| 0.0473 | 799.1 | 0.712 | 817.4 | 1.268 | 837.9 | 1.569 | 113 |
| 0.0745 | 833.2 | 0.739 | 847.6 | 1.222 | 876.9 | 1.680 | 108 |

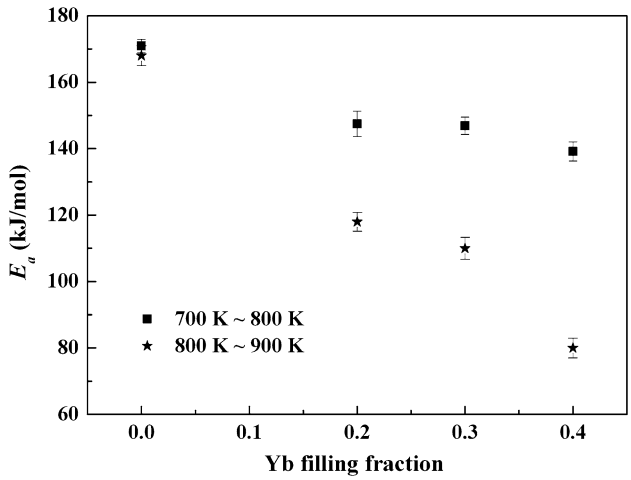


Fig. 7. Oxidation activation energy as a function of Yb filling fraction for $Yb_yCo_4Sb_{12}$ over different temperature ranges.

$Co_4Sb_{12}$ framework, which reduce the stability of filled skutterudites in air. Antioxidation protection is therefore necessary for real application of filled skutterudites in thermoelectric generators. $E_a$ values for all filled samples are lower at 800 K to 900 K than at 700 K to 800 K. This is due to the formation of new oxides and generation of microcracks at higher temperature. Also, this difference is even larger in filled samples with higher Yb content. Considering the unchanged $E_a$ for unfilled $Co_4Sb_{12}$, it is clear that the Yb filling is the reason for the abrupt decrease of $E_a$ at high temperature. Further systemic studies are needed to understand this phenomenon fully.

## CONCLUSIONS

The oxidation behavior of filled skutterudites $Yb_yCo_4Sb_{12}$ in air is studied. $Yb_yCo_4Sb_{12}$ oxidation starts at temperature above 650 K. The oxidation process consists of two stages at different temperature ranges. Firstly, dense oxide layers composed of $Yb_2O_3$, $Sb_2O_3$, $\alpha$-$Sb_2O_4$, $\beta$-$Sb_2O_4$, $CoSb_2O_4$, and $CoSb_2O_6$ are formed on the sample surface, blocking further penetration of oxygen into the bulk. Secondly, microcracks appear in the oxide layers and skutterudite matrix due to the CTE mismatch. Accelerated oxygen diffusion leads to continuous, fast oxidation of skutterudite, contributing eventually to the formation of a bilayer oxide structure. The overall oxidation can be described through the repetition of: dense layer formation → stress release → microcrack formation → self-repair → dense layer formation. The filled skutterudites have lower activation energy $E_a$ than unfilled $Co_4Sb_{12}$. With increasing Yb filling fraction, $E_a$ decreases monotonically. The high oxygen affinity of Yb and the weak bonding between Yb and the $Co_4Sb_{12}$ framework are the main reasons for the low $E_a$ in $Yb_yCo_4Sb_{12}$ filled skutterudites.

## ACKNOWLEDGEMENTS

This work was supported by the National Natural Science Foundation of China (Contract Nos. 5097 2158, 51004096, and 51102260) and the Shanghai Committee of Science and Technology, China (Grant No.10JC1400500).

## REFERENCES

1. G.A. Slack, *CRC Handbook of Thermoelectrics* (Boca Raton: CRC, 1995).
2. T. Kajikawa, *J. Electron. Mater.* 38, 1083 (2009).
3. J.P. Fleurial, *JOM* 261, 79 (2009).
4. B.C. Sales, K.A. Gschneidner, J.C. Bunzli, and V.K. Pecharsky, eds., *Handbook on the Physics and Chemistry of Rare Earths*, Vol. 33 (Amsterdam: Elsevier, 2003), pp. 1–34.
5. J. Yang and T. Caillat, *MRS Bull.* 31, 224 (2006).
6. C. Uher, *Proceedings of the 21st International Conference on Thermoelectrics* (IEEE, Piscataway, NJ, 2001), p. 35.
7. L.D. Chen, T. Kawahara, X.F. Tang, T. Goto, T. Hirai, J.S. Dyck, W. Chen, and C. Uher, *J. Appl. Phys.* 90, 1864 (2001).
8. P.F. Qiu, J. Yang, R.H. Liu, X. Shi, X.Y. Huang, G.J. Snyder,W. Zhang, and L.D. Chen, *J. Appl. Phys.* 109, 063713 (2011) [and reference therein].
9. X. Shi, S. Bai, L. Xi, Jiong Yang, W. Zhang, L. Chen, and J. Yang, *J. Mater. Res.* 26, 1746 (2011) [and references therein].
10. X. Shi, J. Yang, J.R. Salvador, M.F. Chi, J.Y. Cho, H. Wang, S.Q. Bai, J.H. Yang, Q. Zhang, and L.D. Chen, *J. Am. Chem. Soc.* 133, 7837 (2011).
11. Y.J. Xue, K.G. Liu, J.H. Li, and N. Chen, *Mater. Res. Bull.* 40, 1172 (2005).
12. R. Hara, S. Inoue, H.T. Kaibe, and S. Sano, *J. Alloys Compd.* 349, 297 (2003).
13. J. Leszczynski, A. Malecki, and K.T. Wojciechowski, *Proceedings of 5th European Conference on Thermoelectrics* (IEEE, Odessa, Ukraine, 2007), p. 50.
14. E. Godlewska, K. Zawadzka, A. Adamczyk, M. Mitoraj, and K. Mars, *Oxid. Met.* 74, 113 (2010).
15. D.G. Zhao, C.W. Tian, S.Q. Tang, Y.T. Liu, and L.D. Chen, *J. Alloys Compd.* 504, 552 (2010).

16. A.C. Sklad, M.W. Gaultois, and A.P. Grosvenor, *J. Alloys Compd.* 505, L6 (2010).
17. J. Leszczynski, K.T. Wojciechowski, and A.L. Malecki, *J. Therm. Anal. Calorim.* 105, 211 (2011).
18. M. Imaoka, H. Hasegawa, and S. Shindo, *J. Ceram. Soc.* 77, 263 (1969).
19. Y.S. Touloukian, R.W. Powell, C.Y. Ho, and P.G. Klemens, *Thermophysical Properties of Matter*, Vol. 13 (The TPRC Date Series, 1971), p. 435.
20. O. Kubashevski, C.B. Alcock, and P.J. Spencer, *Materials Thermochemistry* (Oxford: Pergamon, 1993).
21. N.A. Asryan, A.S. Alikhanyan, and G.D. Nipan, *Inorg. Mater.* 40, 720 (2004).
22. Z.L. Zhu, D.L. Yang, Y.Q. Guo, Q.Q. Liu, Z.S. Gao, and X. Hu, *Physica C* 383, 169 (2002).
23. D.L. Yang, H.W. Sun, H.X. Lu, Y.Q. Guo, X.J. Li, and X. Hu, *Supercond. Sci. Technol.* 16, 576 (2003).